# Chapter 6

# Colorimetric detection of picric acid using silver nanoparticles modified with 4-amino-3-hydrazino-5-mercapto-1,2,4-triazole

## 6.1 Introduction

Shape designed metallic nanoparticles formulation is a versatile area in present scenario for both industrial as well as academic interests. When bulk size of metals reduced to nano size particles, various interesting properties appeared which are improved from bulk material and allowed interesting applications in numerous areas [Ferraris et al., 2016; Parashar et al., 2014; Patra et al., 2014]. In past few years, various noble metal nanoparticles have been extensively studied for their outstanding properties and their possible applications in, catalysis, biological labeling, surface enhanced Raman scattering, microelectronics, energy conversion, sensing, biological, optical, and magnetic devices etc [Hamed et al., 2010; Matsuhisa et al., 2017; Ahmed et al., 2016; Li et al., 2015]. A lot of research work has been dedicated to the synthesis of stable dispersion for nanoparticles of gold, silver and other metals [Chettri et al., 2017; Roy et al., 2014]. Silver nanoparticles having different size and morphology have fascinated interest because silver shows the maximum thermal and electrical conductivities among other metals [Gupta et al., 2014]. As we know that the synthesis of Ag nanoparticles with definite shape and controlled dimensions has difficult than other metal nanoparticles owing to the great reactivity of silver compounds with good relative abundance, essential physical properties, and low cost [ Aragay et al., 2012]. A lot of reports are exist in the literatures to synthesize silver nanoparticles by using silver salt as a precursor [Lu et al., 2017]. In the current work we executed novel route for synthesis of nanoparticles of silver by using sodium borohydrate as reducing agent, which have well-known complexation with silver as described in the existing literature. Here we report synthetic and simple protocol for fabricating stable silver nanoparticles,

with quantitative yield. The purity, stability, and yield are considerably improved than other nanoparticles. A framework of reaction between AHMT and silver ions has been proposed here, we found scarcely any discussions/evidence of such scheme for synthesis of silver nanoparticles by using AHMT as capping agent and utilization as a colorimetric sensing of Picric acid (PA). Nanomaterials that improve catalytic properties have been deliberated, mainly towards the development of materials for sensing, catalysis, and electrochemical applications [Mahato et al., 2016]. In the present study nano silver particles are discovered for the trace sensing of picric acid.

In the perspective of environmental protection and human health, a number of efforts have been provided to quick detection of aromatic nitro compounds. Picric acid (PA) 2,4,6-trinitrophenol, is a significant nitro compound, and frequently used in pharmaceutical, leather, landmines and dye industries for decades [Maiti et al., 2017]. Nevertheless, the wide use of picric acid has brought a chain of disturbing problems. This compound is a leading environmental pollutant causing the contamination of aquatic and soil systems when it is exposed into environment [Ahmed et al., 2017]. Furthermore, PA is a strong allergen and irritant which may cause several health problems such as anemia, abnormal liver functions and skin irritation [Maity et al., 2017]. Additionally, in metabolism PA converts into its by-product 2-amino-4,6-dinitrophenol, which have ten times additional mutagenic activity than picric acid . Thus, rapid and sensible detection of picric acid is essential for protecting human health and monitoring environmental pollution [Xia et al., 2017]. Numerous methods, including capillary electrophoresis, gas chromatography, spectrophotometry and membrane electrode technique, have been reported for the quantification of PA. Still these methods lack good sensitivity and suffering from various disadvantages as high operational cost, tedious pretreatment of sample, sophisticated instrumentation and long

analysis time [Nagarkar et al., 2013; Nagarkar et al., 2015]. In this view, it is immediately desired to formulate a simple, field-applicable, and low-cost sensor for convenient and reliable quantification of PA. Accordingly, colorimetric techniques have fascinated excessive attention because of their rapidness, simplicity, convenient visual detection, short response time and great sensitivity in the quantification of analyte [Parmar et al., 2016; Di et al., 2017]. We have established the Colorimetric sensing of picric acid by AHMT capped silver nanoparticles (Ag@AHMT Nps) which shows nanomolar detection limit which is much better than other existing spectrophotometric determination of picric acid [Zhang et al., 2017]. Such low detection *via* colorimetric method is credited to catalytic efficacy of nano materials which mostly based on the surface/volume ratio of nanomaterials and the interactions between the analyte and material, also eased electron transfer support the improved sensitivity for quantification of PA. Though, this developed method is easy to handle, highly sensitive and low-priced for detection of picric acid with sensitivity 0.045 ng/mL and detection limit 0.13 nM.

## 6.2 Experimental section

### 6.2.1 Materials

Silver salt ($AgNO_3$), 4-amino-3-hydrazino-5-mercapto-1,2,4-triazole (AHMT), Sodiumborohydrate, Picric acid, were kindly supplied by sigma Aldrich USA. All glassware cleaned by using aqua regia (3: 1, HCl–$HNO_3$) after that wash with ultrapure water and ethanol (Merck India). All materials are of analytical grade reagents and applied without additional purification. Picric acid sample solution was freshly prepared by using doubly deionised water.

### 6.2.2 Instrumentation

The Ag@AHMT nanoparticles were characterized by UV–Visible by using Epoch 2, microplate reader Biotech, USA, spectrophotometer in 1cm (path length) quartz cuvette. The FT–IR spectrum was executed on KBr in range of 4000 to 400 $cm^{-1}$ performed by Perkin- Elmer 783, spectrometer. Crystalline nature of Ag@AHMT nanoparticles were examined by X-ray diffraction, in range of 35° to 80° by using Miniflex 600 diffractometer (Kα =1.54056 Å, Cu–Kα radiation, scan rate = 3°/min). For the elemental analysis of Ag@AHMT nanoparticles X–ray photoelectron spectrometer (XPS), was used and performed by Kratos, analytical instrument, Shimadzu group company, Amicus, XPS, UK, with Mg (Kα = 1.254 Å) radiation. The high HR- SEM was executed by Nova-Nano-SEM 450 FEI (Netherlands). High Resolution Transmission Electron Microscopy (HR-TEM), The Energy Dispersive X-ray (EDAX) and EDS mapping were performed with FEI, TECHNAI ,$G^2$ 20 TWIN, Czech Republic, with accelerating voltage of 200 keV on copper grid (carbon coated) modified with Ag@AHMT nanoparticles solution. Zeta potential of Ag@AHMT was executed by Nanoparticles Analyzer SZ-100 (Japan).

### 6.2.3 Experimental route for silver nanoparticles Synthesis

The aqueous solution of $AgNO_3$ (10 mM), sodiumborohydride (60 mM) and the AHMT (1 mM) were prepared. Further, sodiumborohydride solution, a reducing agent was added dropwise into the solution of $AgNO_3$ and AHMT with stirring for 1 h at room temperature and atmospheric pressure. A Yellow color solution of silver nanoparticles obtained and the resulting solution was analyzed by UV-Vis, FT-IR, XRD, XPS, Zeta, HR-SEM, HR-TEM, EDAX, and EDS mapping.

## 6.3 Results and discussion

### 6.3.1 Time dependent study for the formation of AHMT capped silver nanoparticles

The kinetics of initial stage of the formation of Ag@AHMT nanoparticles was analyzed by UV-visible spectroscopy. The initial stages of the formation of silver nanoparticles when nucleation dominated was examined through UV-Vis spectra (Figure 6.2) and feature progressively produces as a strong peak at ~410 nm resembling to characteristic surface plasmon resonance band of silver nanoparticles [John Xavier et al., 2014]. AHMT molecules influence the rate of reaction or nucleation for the silver nanoparticles formation. Here, AHMT functions as capping agent for selectively bind silver nanoparticles and possible reaction mechanism for the formation of the silver nanoparticles has been proposed (Figure 6.1). AHMT adsorbed on the surface of the silver nanoparticles via attachment with sulphur atom present in its assembly which protect silver nanoparticles for agglomeration [Wang et al., 2013], thus successfully leading to the formation of Ag@AHMT nanoparticles.

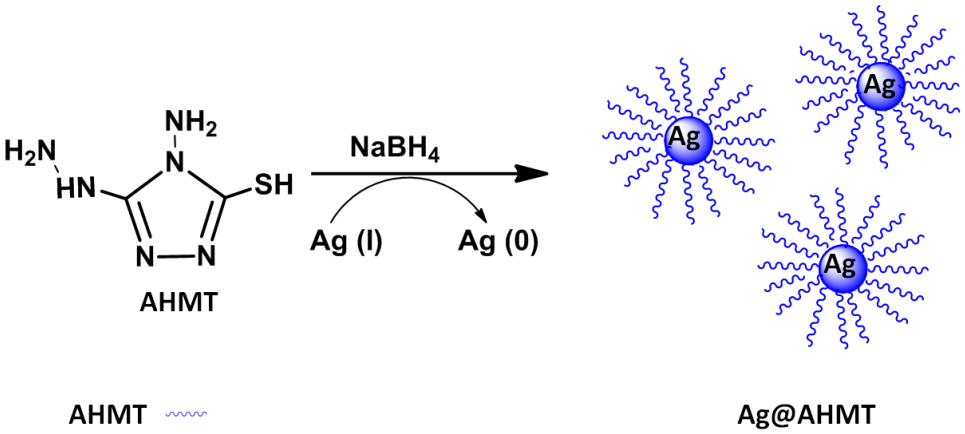


**Figure 6.1** Schematics of Ag@AHMT synthesis.

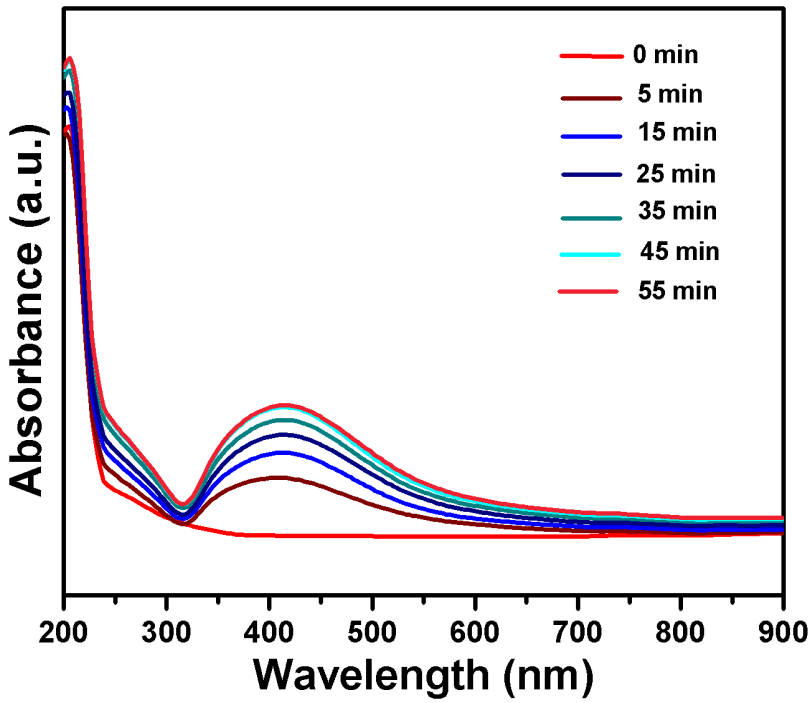


**Figure 6.2** Time dependent study for the formation of Ag@AHMT nanoparticles by UV-Vis spectrum, (at 0 min, 5 min, 15 min, 25 min, 35 min, 45 min, 55 min)

### 6.3.2 Materials characterizations

The synthesized Ag@AHMT nanoparticles were characterized and studied by UV-Vis absorption, XRD, FT-IR, XPS, TEM, HR-SEM, EDS mapping and zeta potential talk over one by one.

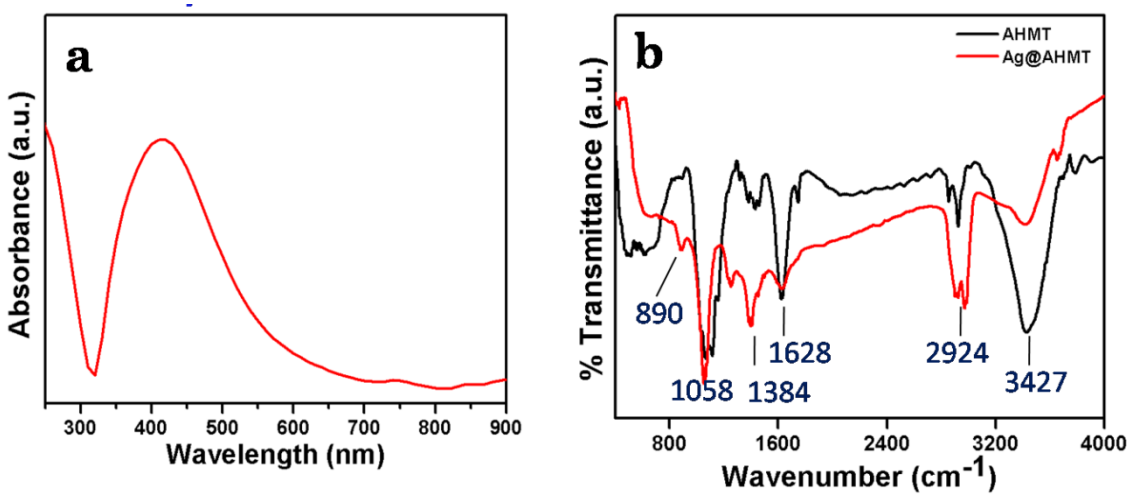


**Figure 6.3** (a) UV-Vis spectra (b) FT-IR Spectra of AHMT and Ag@AHMT nanoparticles**.**

The formation of AHMT capped (Ag@AHMT) silver nanoparticles were confirmed and optimized by UV-Vis spectrum as shown in Figure 6.3a showing surface plasmon resonance at 410 nm resembles to characteristic SPR band of nano silver of size in the range 4 nm to 15 nm [Mott et al., 2017]. This investigation also verified by HR SEM and TEM analysis. The FT-IR spectrum of AHMT and Ag@AHMT nanoparticles are shown in Figure 6.3b, the strong bands at 3427, 2924 and 1628 corresponds to -NH, N-H adjacent to C=S and N=N stretching respectively. Further the band at 1384 $cm^{-1}$ is assigned for C=C bond stretching. Additionally the vibration at 1116 & 1066 $cm^{-1}$ resulted due to N-C-S and C=S stretching in AHMT get shifted towards lower wavelength at 1058 & 890 $cm^{-1}$ in Ag@AHMT confirming the capping of silver nanoparticles with thiol of AHMT, thus leading to the formation of silver nanoparticles by surface-bound AHMT.

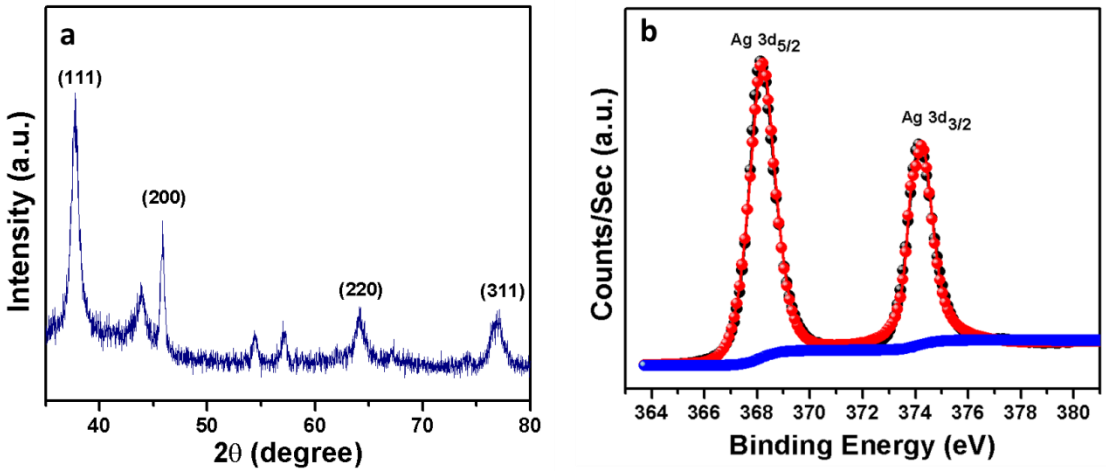


**Figure 6.4** (a) X-ray Diffraction of Silver nanoparticles indexed from JCPDS (CAS no. 7440-22-4) file and (b) XPS spectrum of Ag (0).

Further, X-ray diffraction was carried out to approve crystalline nature of Ag@AHMT nanoparticles and XRD spectra obtained is shown in Figure 6.4a. The XRD pattern indicated four strong peaks in whole spectrum of 2 theta, ranging from 35 to 80. The 2 theta peaks values of about 38.11◦, 44.27◦, 64.43◦ and 77.47◦, were observed [Phanjom

et al., 2015]. A comparison of observed XRD data with the standard XRD spectrum confirmed that Ag@AHMT nanoparticles formed in the experiment were of face centered cubic (FCC) type nanoparticle crystals, corresponding to [111], [200], [220] and [311], respectively [JCPDS (CAS no. 7440-22-4)]. Again the chemically reduced Ag indicate peaks in the spectrum of XPS as shown in Figure 6.4b at 368.1 and 374.1 eV which can be assigned to Ag (0) 3d5/2 and Ag (0) 3d3/2 respectively, this confirms that silver is in zero oxidation state (reduced silver) also confirmed by EDAX studies [Fratoddi et al., 2017]. From the experimental results we see that Sodium borohydride reacts with the silver ions through the redox reaction in presence of AHMT yielding silver colloids and rest of AHMT. Here AHMT get adsorb on Ag (0) surface through sulphur atoms [Mavani et al., 2013].

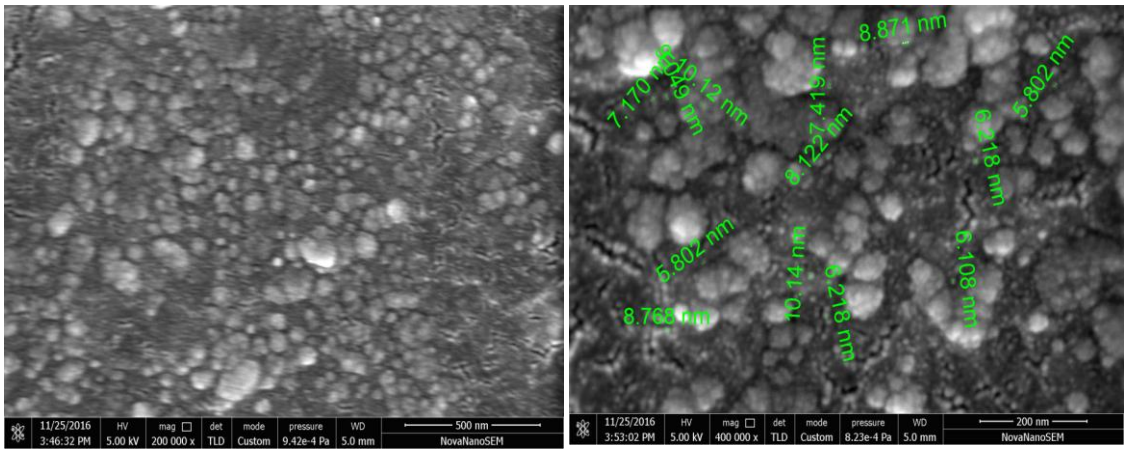


**Figure 6.5** HR SEM of Ag@AHMT nanoparticles.

The surface morphology of Ag@AHMT nanoparticles were analyzed by HR SEM images as shown in Figure 6.5, where distribution shows that AHMT capped silver nanoparticles are uniformly dense with homogenous distribution. Average size lies below 10 nm also established by TEM images (Figure 6.6a, 6.6b and 6.6c) explores that the size of silver nanoparticles lies in 4-10 nm range. The average particle size

distribution of Ag@AHMT nanoparticles were calculated by standard Image J software (Figure 6.7) which shows average size of nanoparticles lies between 4-10 nm. The corresponding selected-area electron diffraction pattern (SAED) illustrates the Ag@AHMT nanoparticles formed were the silver nano crystal with Scherrer rings indexed as [111], [200], [220], and [311] planes of face-centered cubic (FCC) silver lattice (Figure 6.6d). Furthermore, the reduction of Ag is also confirmed by EDAX as shown in Figure 6.8 and EDAX spectrum reveals that Ag@AHMT nanoparticles contain N, C, S and Ag elements. From EDAX spectrum it is evidenced that existence of strong peak signal near 3 keV was owing to SPR of metallic Ag [Kalimuthu et al., 2008]. Additionally, the relative location of Ag, C, S and N within the particle is demonstrated via EDS Mapping. Here the Ag region is presented in golden area and the C, S and N region is shown in purple, white, blue areas as shown in Figure 6.9. The overlapping maps evidenced that the Ag is located in the maximum area of the particle while the remaining atoms are scattered. The collective EDS mapping and STEM studies provide definitive evidence of the Ag nanoparticles [Shankar et al., 2012].

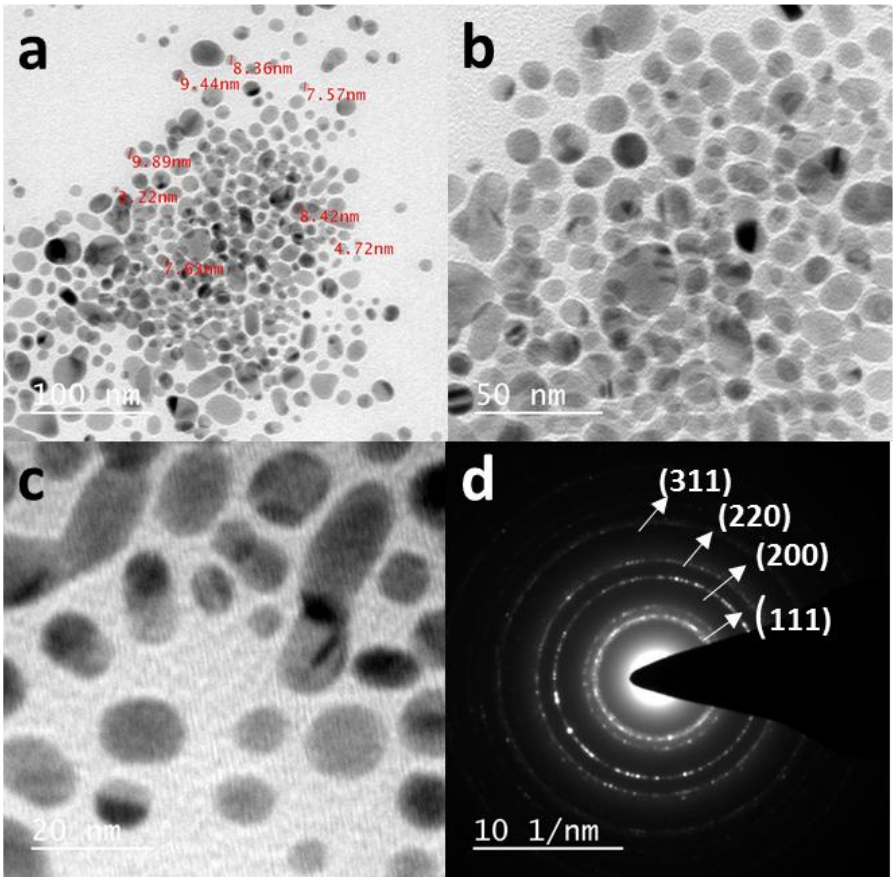


**Figure 6.6** TEM images of Ag@AHMT nanoparticles (a,b,c) and corresponding SAED pattern (d).

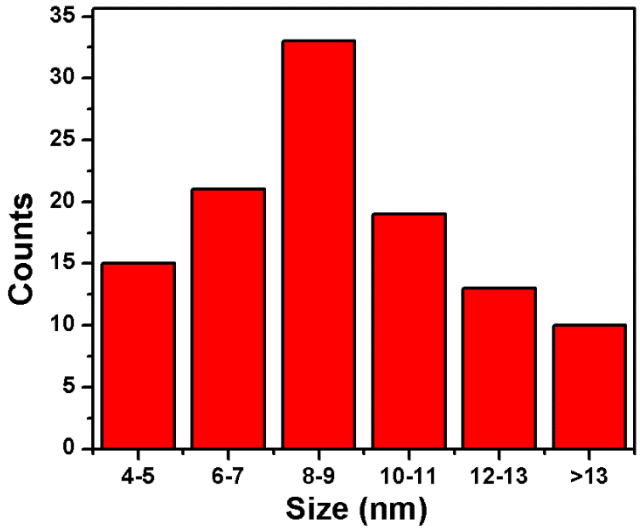


**Figure 6.7** Particle size distributions of Ag@AHMT nanoparticles.

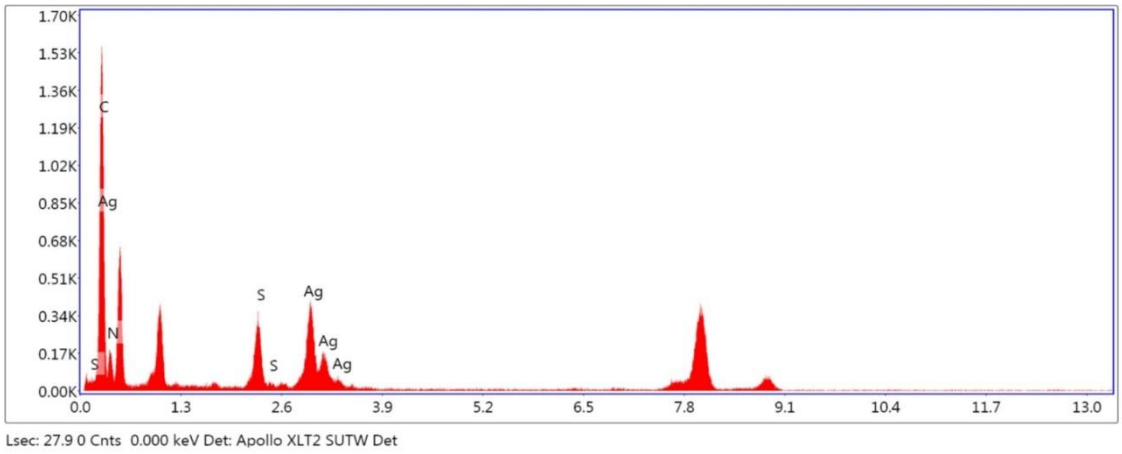


**Figure 6.8** EDAX of Ag@AHMT nanoparticles.

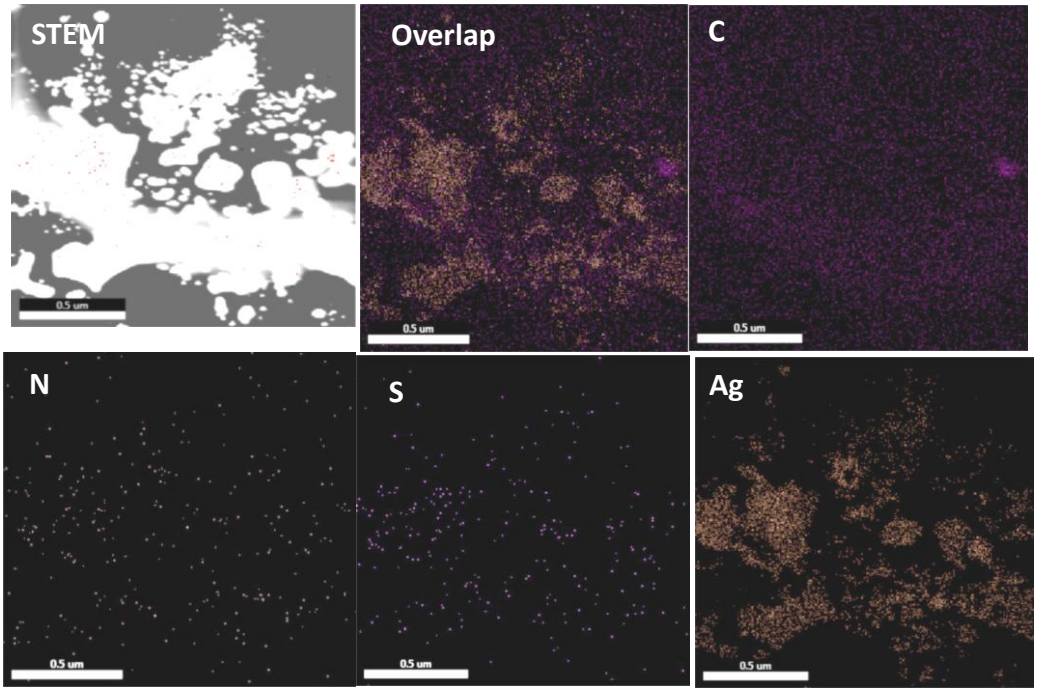


**Figure 6.9** EDS Mapping of Ag@AHMT silver nanoparticles.

After that dispersion stability of synthesized Ag@AHMT nanoparticles in water is investigated spectroscopically through zeta potential measurement that specifies the changes appeared on the Ag@AHMT nanoparticles surface with time. The zeta potential value of the prepared Ag@AHMT nanoparticles is +36.2 mV compared to

naked silver nanoparticle (-20.6 mV) **(**Figure 6.10) indicates the high stability of Ag@AHMT in water[Tiwari et al., 2015]. To monitor the stability of the Ag@AHMT Nps, UV-Vis measurements were performed after 30 days of synthesis as evidences in Figure 6.11. The negligible shifting of the SPR band confirmed the strong binding affinity of AHMT towards silver nanoparticle. The designed Ag@AHMT are investigated and explored for the colorimetric assay of environmental hazardous pollutant picric acid.

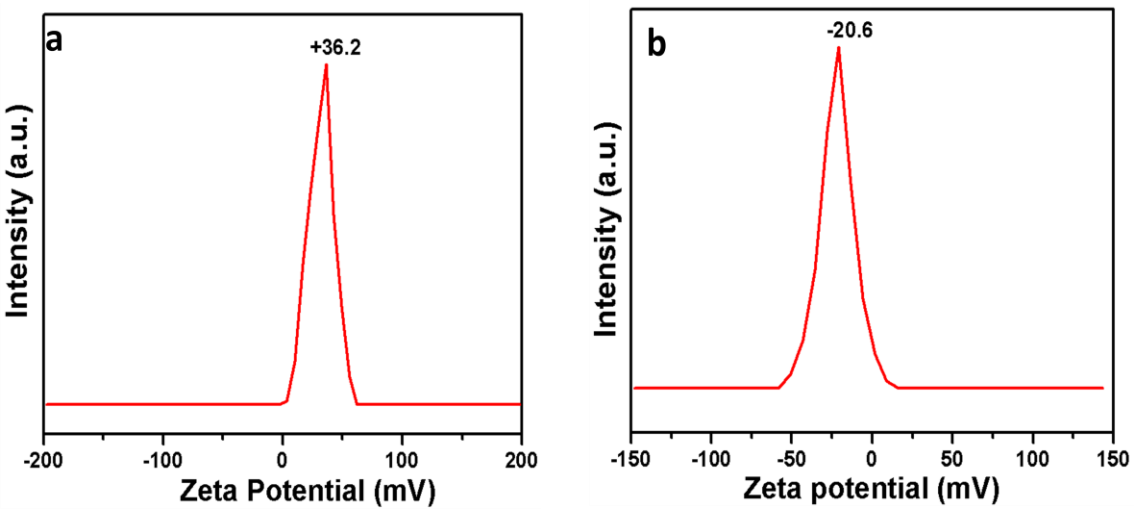


**Figure 6.10** surface Zeta potential graphs of Ag@AHMTnanoparticles (a) and naked silver nanoparticles (b).

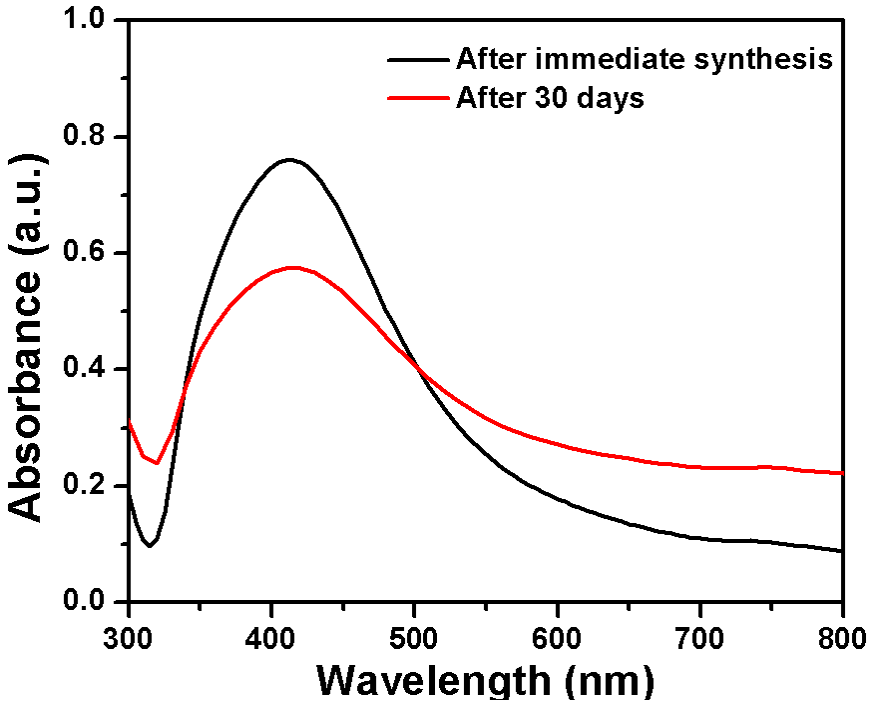


**Figure 6.11** Stability of Ag@AHMTNps checked by UV-Vis.

### 6.3.3 Application of Ag@AHMT in colorimetric detection of picric acid

The developed Ag@AHMT is utilized for the colorimetric detection of hazardous environmental pollutant picric acid. Ag@AHMT exhibits strong surface plasmon band at 410 nm (Figure 6.12). Upon concomitant addition of picric acid it shows a blue shifting indicating interaction between the picric acid and Ag@AHMT. This shift can be visualized through naked eye as the light yellow color of Ag@AHMT changes into brownish yellow. Further addition of Picric acid shows strong blue shifting. Color change of the Ag@AHMT Nps solution with the different concentration of picric acid has also provided (Figure 6.13). There must be hydrogen bonding between -OH, $-NO_2$ of picric acid and –NH, $-NH_2$ of Ag@AHMT. Besides hydrogen bonding, possibly there is formation of charge transfer complex between electron rich capping agent (AHMT) and electron deficient picric acid which induces the agglomeration of silver nanoparticles [Bouduban et al., 2017] and thus leading to the blue shift in the absorption

spectra due to interparticle plasmon coupling [Zhu et al., 2008] as shown in the schematic (Figure 6.15). The picric acid addition has strongly affected the morphologies of Ag@AHMT as evidenced by TEM experiments (Figure. 6.14). The Ag@AHMT Nps are well dispersed while addition of picric acid causes aggregation. The UV plot for the successive addition of PA (Figure 6.12 a) and the corresponding calibration plot (Figure 6.12 b) shows linear response of picric acid concentration with sensitivity 0.045 ng/mL (slope of the curve) and limit of detection 0.13 nM calculated from the formula 3xStandard Deviation/slope.

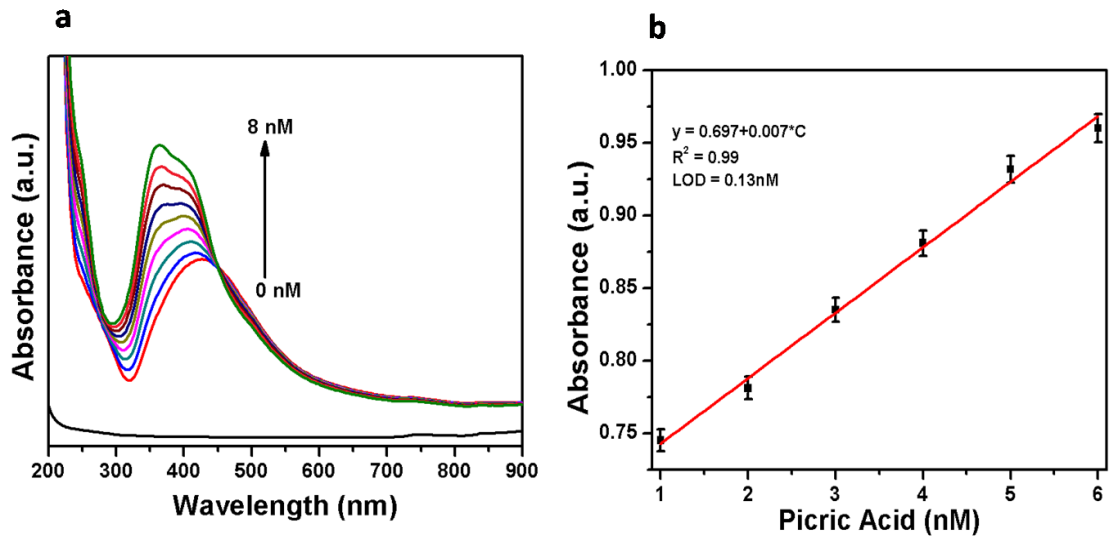


**Figure 6.12 (a)** Colorimetric sensing with different concentration of picric acid (1, 2, 3, 4, 5, 6, 7, 8 nM). **(b)** Calibration curve of colorimetric sensing with different concentration of picric acid (1, 2, 3, 4, 5, 6, 7, 8 nM).

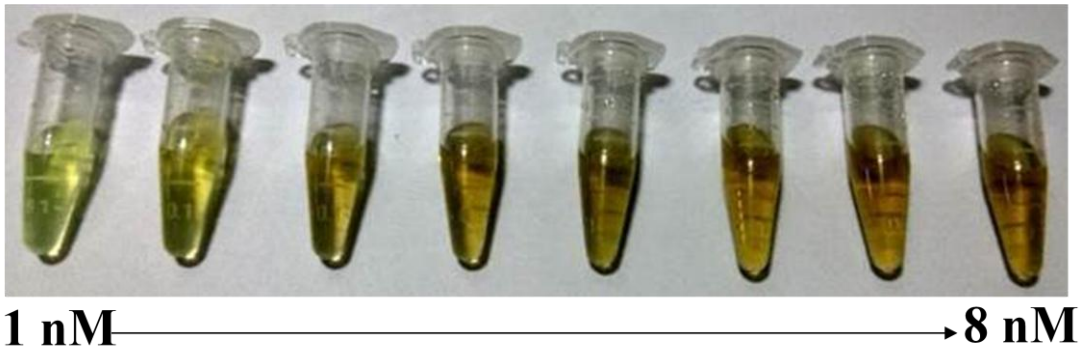


**Figure 6.13** Photographs showing the color-change during colorimetric sensing of Picric acid.

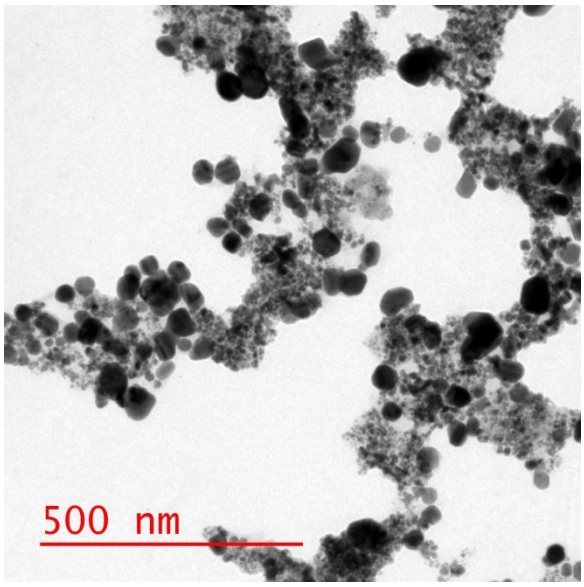


**Figure 6.14** TEM images of Ag@AHMT+Picric acid.

The schematic shows the formulation of Ag@AHMT Nps and colorimetric assay of picric acid, the possible mechanism for the highly sensitive detection is presented in the Figure 6.15. Herein the colorimetric detection is possible through the H-bonding and charge transfer complex formation leading to the aggregation causing blue shift.

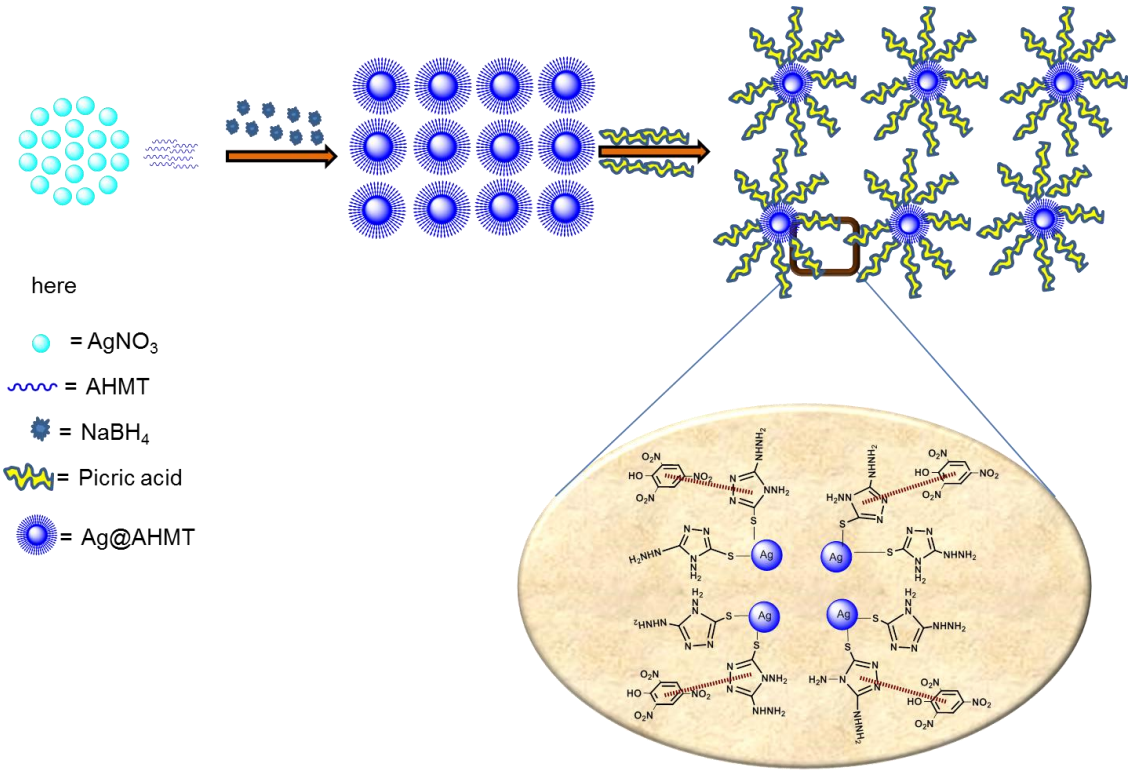


**Figure 6.15** The schematic presentation of formation of Ag@AHMT nanoparticles and interaction with picric acid.

### 6.3.4 Repeatability test for proposed colorimetric system

The reproducibility was verified by conducting both intra-day (0, 2, 4 and 6 hrs) and inter-day (0, 1, 2 and 3 days) repeatability test of picric acid detection (ranges of the concentrations from 1 nM to 8 nM of picric acid). Figure 6.16 (a) and (b) are shows the consistent repeatability results of the intra-day and inter-day test of picric acid respectively.

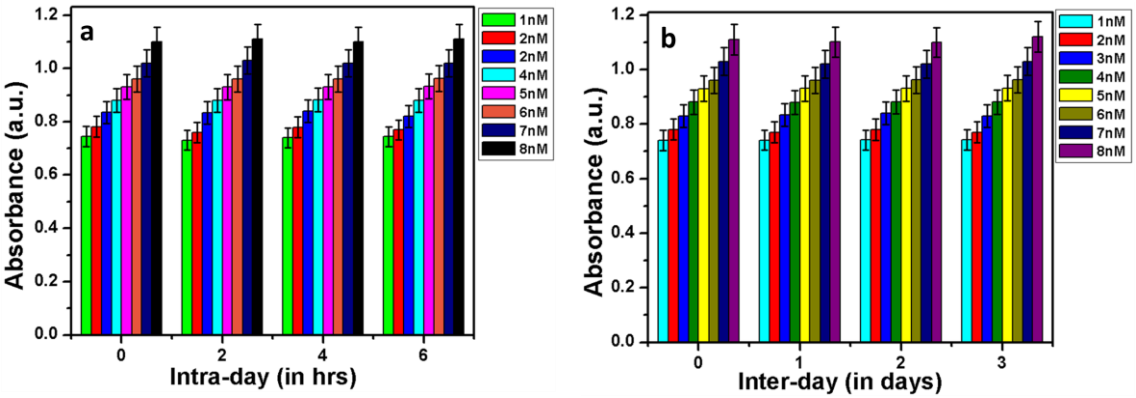


**Figure 6.16** Intra-day (a) and inter-day (b) repeatability test for the detection of picric acid (concentration ranges from 1nM to 8 nM).

## 6.4 Conclusions

This article explores the formulation of highly stable and homogenously distributed Ag@AHMT. The key for the success of synthesis and stabilization of Ag@AHMT is the strong interaction between Ag and S atoms of AHMT which is in consistent with the various results of this article. The developed Ag@AHMT is explored for the highly sensitive ultra-trace detection of hazardous environmental pollutant picric acid. The sensing platform exhibits instant response toward variation in picric acid concentration through change in color from light yellow To brownish yellow and can be visualized via naked eye. Herein, the highly sensitive assay is possible in the light of strong H-bonding and charge transfer complex formation which affect catalytically the surface plasmon resonance of Ag@AHMT Nps and shows linear response towards picric acid concentration in dynamic range 1 nM to 8 nM with the sensitivity 0.045 ng/mL and limit of detection 0.13 nm. This approach suggests a highly sensitive, enzymeless, mediatorless colorimetric assay and will open nano avenues in the area of naked eye sensing device fabrication.